Cavity Ripples Observed during the Impact of Solid Objects into Liquids

Torben Grumstrup,[1,*] Joseph B. Keller,[2] and Andrew Belmonte[1,†]

[1]*W. G. Pritchard Laboratories, Department of Mathematics, Pennsylvania State University, University Park, Pennsylvania 16802, USA*
[2]*Departments of Mathematics and Mechanical Engineering, Stanford University, Stanford, California 94305, USA*

(Received 3 April 2007; published 12 September 2007)

We report the experimental observation of a well-defined rippling of the air cavity entrained by a rapidly moving solid object entering the free surface of a liquid (water or ethanol). The ripples are fixed in the lab frame, and begin just after the pinch-off (deep seal) of the cavity, simultaneous with the acoustic emission. This acoustic resonance corresponds approximately to the Minnaert frequency for volume oscillations of the bubble. We present an irrotational model which explains the ripples as a spatial rectification of these volume oscillations by the surface of the moving object.

DOI: 10.1103/PhysRevLett.99.114502 PACS numbers: 47.55.dd, 47.55.dp

The everyday flow of liquids and air can generate audible sound: the gurgling of a brook [1] or the roar of ocean waves, ''the underwater noise of rain'' [2,3]. A simple demonstration is provided by dropping a coin into a cup of water. The plunk sound is produced by the pinch-off of the cavity created behind the object as it descends into the fluid; it can also produce a large upward splash, or ''Worthington jet'' [3–5]. There have been many studies of cavity formation during impact [6–9], including the related case of a drop or liquid column striking a free liquid surface [3,10,11]; recent studies have focused on the shape or scaling of the cavity before pinch-off [12,13]. The sound one hears is produced by volume oscillations of the air entrained by the cavity closure—a transient version of the acoustically driven bubble oscillations responsible among other things for sonoluminescence [14]. Bubbles attached to stationary flat walls will also oscillate, either alone [15] or in patterned arrays [16].

In this Letter we present a surprising phenomenon: well-defined surface waves or cavity ripples which appear on long entrained bubbles attached to a rapidly moving solid object after it has impacted a free fluid surface. These ripples are acoustic in origin, initiated by the acoustic perturbation of the cavity pinch-off. As far as we know, these ripples are mentioned only twice in the literature [4,5], the first being Worthington.

To study the dynamics of long entrained air bubbles we drop different objects into a large glass tank filled with water, and observe the results with a high-speed digital video camera (Phantom v5.0, Vision Research) operating at about 2000 frames/s, with an exposure time of 45 μs. Projectiles include steel, nylon, teflon, and delrin spheres of different diameters ($d = 1/8$–$1\frac{1}{2}$ in.), brass hemispheres ($d = 1/2$ in.), and cones ($d = 1/2$ in., half-angle 45°). These objects fall under gravity into a $62 \times 42 \times 32$ cm^3 glass-sided aquarium tank filled with tap water. The tank does not interfere with cavity expansion or pinch-off for any of the experiments reported. Underwater acoustic emissions are detected by a Celesco Industries LC-10 hydrophone, which has a flat response curve from 0.1 Hz to 4 kHz; pressure data are acquired with an Agilent 54622A digital oscilloscope. A vacuum holding mechanism is mounted above the tank to release objects without imparting spin, which can strongly affect the cavity dynamics [17].

The impact of an object of spatial size d into a liquid at velocity U_i is usually characterized by the nondimensional Froude number $\mathrm{Fr} = U_i^2/gd$, where g is the gravitational acceleration [6,18]. However, the object must also have sufficient roughness to produce a cavity at all [5,19]. Our stainless steel spheres are manufactured with a smooth chrome finish, which can be flaked off by heating the sphere until red hot and then quenching it in cold water, leaving a less smooth surface. All steel spheres we used are roughened in this way. Drop heights range from 10–150 cm, with impact speeds $U_i = 1$–5 m/s corresponding to typical Reynolds numbers $\mathrm{Re} \sim 6 \times 10^4$ and $\mathrm{Fr} \simeq 100$. For the air inside the bubble typical Weber numbers are $\mathrm{Wb} \simeq 3 \times 10^3$, and $\mathrm{Re} \simeq 4 \times 10^3$.

Impact-produced cavities are known to close in two different ways [18], the first driven by air flow into the cavity, sealing it off near the original surface [20]. The other is known as deep closure, and is driven by hydrostatic pressure, ultimately causing the cavity to collapse near its midpoint [6,21]. This produces the most audible sound of the impact as well as the Worthington jet [20]. The resulting lower segment often remains whole and attached to the projectile; thus the moving projectile entrains a large and possibly long air bubble [19].

Figure 1 shows the cavity ripples produced by a $d = 1/2$ in. steel sphere with $U_i = 4.0$ m/s ($\mathrm{Fr} = 130$, $\mathrm{Re} = 5 \times 10^4$). The ripples begin simultaneously with the deep seal of the cavity (first frame), as a nearly sinusoidal perturbation of the entrained bubble surface originating at the sphere. While the first ripple drifts upward slowly, all subsequent ripples are fixed in the laboratory frame, as can be made apparent by laying a straight edge horizontally across Fig. 1. The cavity surface created before pinch-off is free of ripples. As the sphere descends the newer ripples decrease in amplitude. However, they sometimes

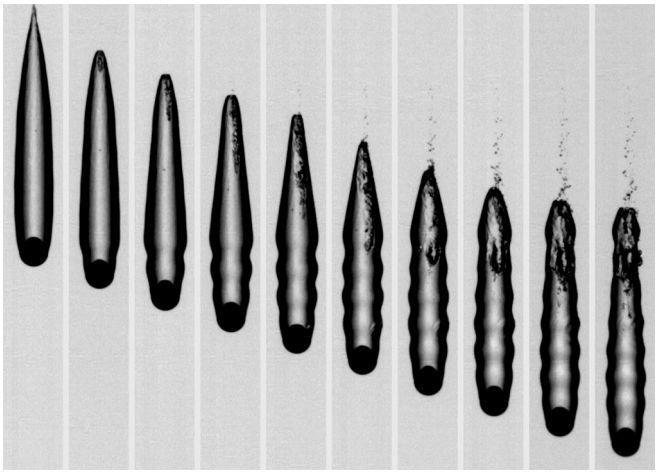

FIG. 1. The onset of rippling after the pinch-off of a cavity formed by a $d = 1/2$ in. steel sphere with impact velocity $U_i \simeq 4$ m/s (Fr = 128, Re = 5.1×10^4, $\Delta t = 3.2$ ms).

induce a spectacularly periodic breakup (see Fig. 2), an effect mentioned by Worthington [5].

For the steel sphere shown in Fig. 1, the rippling wavelength λ is very close to the diameter d; for other steel spheres with the same U_i we find $\lambda \sim d$. However, this does not hold exactly for other projectiles. Figure 3 shows examples of the ripples produced by brass cones, hemispheres, and teflon spheres. The cavity for the teflon sphere is significantly shorter than for steel with the same U_i and d (Figs. 1 and 2). This is partly an effect of the lower inertia of the teflon spheres, which results in a lower speed U_0 at pinch-off than for steel. The rippling is strikingly affected: while $\lambda \sim 0.9d$ for steel spheres, for teflon $\lambda \sim 0.3d$. The ripples also have a more complicated, asymmetric form for both the teflon spheres and the cone (Fig. 3), moreover the two asymmetries are opposite. We do not yet understand these aspects.

Evidence that cavity rippling does not depend on surface tension was obtained by comparing the ripples produced by a $d = 1/2$ in. teflon sphere dropped from $h_0 = 79$ cm into water ($\gamma \sim 73$ dyn cm^{-1}) and into pure ethanol ($\gamma \simeq 22$ dyn cm^{-1}) at the same Fr. We observe very similar ripples in both cases, with slightly different wavelengths ($\lambda = 4.5 \pm 0.3$ mm for water and $\lambda = 5.8 \pm 0.3$ mm for ethanol). The larger λ in ethanol is accounted for by the slightly higher U_0 than in water, since ethanol is less dense than water and the high Re drag is proportional to the fluid density (here Re $\simeq 5 \times 10^4$) [6,22].

What determines the wavelength of the ripples? The linear dependence of λ on d and the decrease in λ for shorter bubbles indicates a volume dependence. This suggests the ripples are acoustic in origin, and related to the resonant volume oscillations of the bubble, initiated by the pressure perturbation of pinch-off. The sound produced during the entry of the projectiles is measured with a hydrophone close to the bubble trajectory. The large-amplitude oscillations begin at the moment of deep seal (~ 22 ms, inset of Fig. 4), decaying slightly until the projectile strikes the bottom of the tank (not shown). For this oscillation the spectrum is narrow, with a dominant frequency $f \simeq 190$ Hz, which is close to the Minnaert frequency based on the bubble diameter. We observe moreover that the product of λ and f is approximately equal to the projectile speed U_0 (Fig. 4), independent of the object density or shape. However, we are unable to obtain data at arbitrarily small velocities: we do not observe ripples for $U_0 < 1$ m/s. The relation $\lambda f = U_0$ means that in the rest frame of the projectile the ripples are purely advected, as if the projectile were an acoustic source which only affects the fluid locally as it flows past.

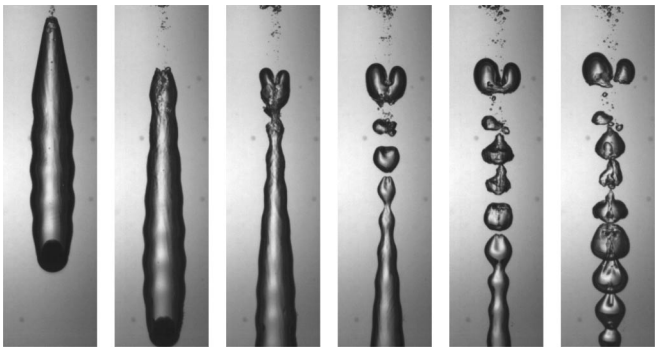

FIG. 2. Ripple-induced breakup of the entrained bubble behind a 1/2 in. diameter steel sphere, $U_i = 4.1$ m/s.

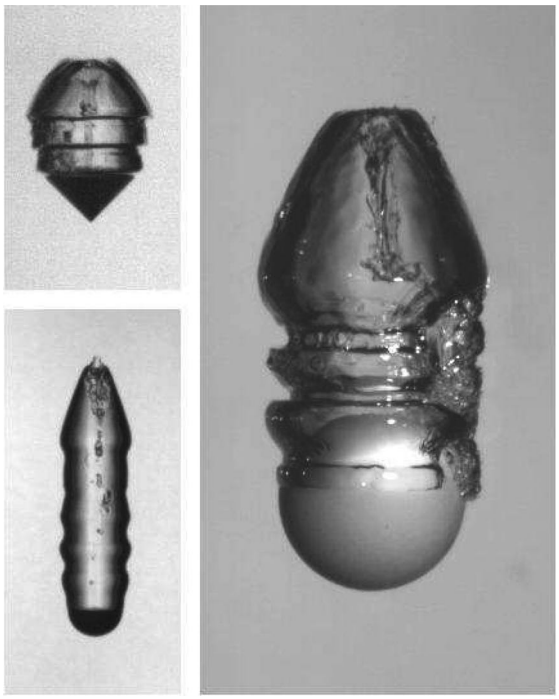

FIG. 3. Cavity rippling behind a brass cone ($d = 1/2$ in., $U_i = 4.5$ m/s), brass hemisphere ($d = 1/2$ in., $U_i = 5.7$ m/s), and teflon sphere ($d = 3/4$ in., $U_i = 4.1$ m/s).

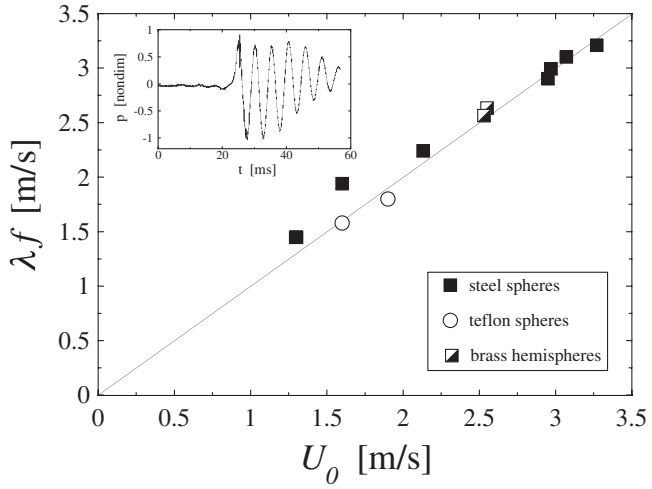

FIG. 4. Plot of the product of the ripple wavelength and acoustic frequency f versus the speed of the sphere. The straight line shows $\lambda f = U_0$. Inset: Pressure oscillations after cavity pinch-off for a 3/4 in. steel sphere ($U_0 = 4$ m/s, Fr = 86).

The earliest mathematical model for bubble dynamics in a fluid was written by Rayleigh [23], for a spherical bubble in an irrotational flow. Later Minnaert derived the resonant frequency of a gas bubble undergoing radial oscillations via physical arguments [1]; this resonance was later shown to be insensitive to bubble shape even for large deformations [24]. For a review of the interwoven progress in experiments and models, see [3].

We base our model on two physical aspects of bubble acoustics: (1) the restoring force due to the compressed gas in a squeezed bubble and (2) the coupling of bubble motion to its fluid environment. The crucial assumption of our model is that the radial displacement of the cylindrical bubble must vanish at the point of contact with the projectile. We assume that an axisymmetric body of maximum cross-sectional radius a_0 enters the water and produces behind it an air-filled cylindrical cavity of the same radius. The cavity pinches off in deep closure at some time $t = 0$, which results in a sudden increase of the air pressure P in the cavity [25], from an ambient p_0 to $P = p_0 + \varepsilon p_1$, where $\varepsilon \ll 1$.

Consider the radially pulsating bubble motion caused by this sudden overpressure. We treat the fluid velocity outside of the bubble as irrotational but not completely incompressible, so that the velocity potential $\phi(r, t)$ satisfies a wave equation outside of the bubble [26] instead of Laplace's equation [27]. We suppose that the cavity length L is large compared to a_0, then the subsequent oscillations of the cavity radius $a(t)$ can be approximated by that of an infinitely long cavity. Such a case was analyzed by Epstein and Keller [28] using the wave equation

$$\phi_{rr} + r^{-1}\phi_r = c^{-2}\phi_{tt} \qquad r \geq a(t) \tag{1}$$

where c is the speed of sound in water, and subscripts denote partial derivatives. The water is assumed to be at rest initially, thus $\phi(r, 0) = 0$ and $\phi_r(r, 0) = 0$ for $r \geq a_0$, also $a(0) = a_0$. The pressure in the water is given by the Bernoulli equation

$$p(r, t) = p_0 - \rho(\phi_t + \phi_r^2/2) \qquad r \geq a(t) \tag{2}$$

where ρ is the density of water. The velocity of the cavity surface must equal the velocity of the water at the surface: $a_t = \phi_r(a, t)$. The pressure must also equal the air pressure P in the cavity, given by the polytropic gas law $PV^\kappa = \text{const}$, where V is the volume and $\kappa = 1.4$ the adiabatic exponent for air. From this we obtain

$$p(a(t), t) = P(a_0)\left[\frac{a_0}{a(t)}\right]^{2\kappa} = (p_0 + \varepsilon p_1)\left[\frac{a_0}{a(t)}\right]^{2\kappa}. \tag{3}$$

Equations (1)–(3) were solved with these boundary conditions in [28] by expanding about the state of rest to first order in ε. For small t they obtained a solution (their Eq. 48) which we rewrite as

$$a(t) = a_0 + \frac{\varepsilon p_1 a_0}{2\kappa p_0}\left[1 - e^{-\alpha t}\left(\cos\omega t - \frac{\alpha}{\omega}\sin\omega t\right)\right]H(t) + O(\varepsilon^2), \tag{4}$$

where H is the Heaviside function, and the damping rate α and frequency ω are [28]

$$\alpha = \frac{\kappa p_0}{\rho c a_0}, \qquad \omega = \left[\frac{2\kappa p_0}{\rho a_0^2} - \left(\frac{2\kappa p_0}{\rho a_0 c}\right)^2\right]^{1/2}. \tag{5}$$

We extend their approach to a long cavity attached to a body moving at speed U_0. Working in the lab frame, we assume the cavity surface is attached to the body at the point $z_0(t) = z_* - U_0 t$ where the body has its maximum radius a_0, and z_* is its location at $t = 0$. Maintaining this attachment means that the radial surface displacement $\eta(z, t)$ must vanish at $z = z_0(t)$. But the spatially independent surface oscillation given in (4) cannot satisfy this condition. Therefore $\eta(z, t)$ must include a "reflected" standing wave $\eta_R(z)$ to cancel the oscillations at the body: $\eta(z, t) = a(t) - a_0 + \eta_R(z)$. The condition $\eta(z_* - U_0 t, t) = 0$ determines the reflected wave to be

$$\eta_R(z) = -\frac{\varepsilon p_1 a_0}{2\kappa p_0}\left\{1 - e^{-\alpha(z_* - z)/U_0}\left[\cos\frac{\omega(z_* - z)}{U_0} - \frac{\alpha}{\omega}\sin\frac{\omega(z_* - z)}{U_0}\right]\right\}H(z_* - z). \tag{6}$$

This reflected wave is the ripple. It has a wavelength $2\pi U_0/\omega$, which explains the experimental relation $\lambda f = U_0$. The standing wave in the model does not extend above the position z_* of the object at pinch-off—represented by the factor $H(z_* - z)$—just as is observed. Also, the ripple amplitude is proportional to the excess pressure perturbation εp_1 produced by pinch-off, and decreases with time due to acoustic radiation (α).

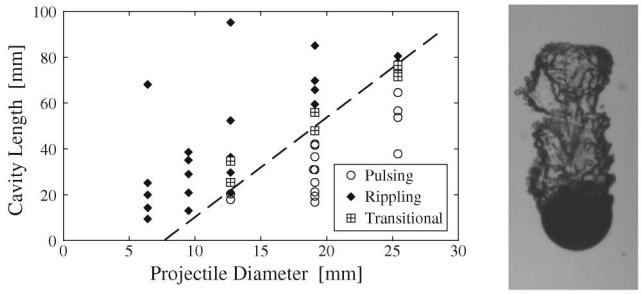

FIG. 5. Left: Dependence of the rippling transition on cavity dimensions for different spheres. The dashed line approximates the transition boundary. Right: The transitional pulsing or rippling state ($d = 3/4$ in. teflon, $U_i = 1.5$ m/s, Fr = 12).

Not all entrained bubbles exhibit rippling. An object which entrains a bubble at a slow enough speed results instead in a pulsing of the whole volume. The bubbles typically have a brainlike texture, indicative of the excitation of many short-wavelength components, unlike rippling [27]. Pulsing generally occurs at lower Fr, but also for shorter cavities, suggesting that rippling requires a minimum aspect ratio (length to width). To investigate this, we correlate the transition to rippling with the cavity length L (here defined as the distance from the point of pinch-off to the center of the body) and the projectile diameter (which sets the cavity width); see Fig. 5. This plot shows the approximate way in which the aspect ratio determines whether a cavity will ripple or pulsate: a line fit to the transitional regime corresponds to a range of aspect ratios from 2–3 (Fig. 5). However the transition is seen only for $d \geq 1/2$ in., so clearly rippling is not simply determined by the aspect ratio. We also observe an intermediate state for which the cavity exhibits a mixture of both rippling and pulsing (Fig. 5). We find moreover that if deep seal does not occur (for whatever reason) then rippling is not observed, even if a long bubble is entrained after surface seal [18]. We do not fully understand the rippling transition, but the requirements seem to be both a large pressure impulse supplied by the deep seal and a long entrained bubble.

We have presented a study of the rippling of an air cavity attached to a rapidly moving solid object (sphere, cone, hemisphere) in both water and ethanol, initiated by the post-impact pinch-off of the cavity. Our potential flow model implies that the ripples are an acoustic phenomenon, due to a standing wave reflected from the projectile surface and defined by $\lambda f = U_0$. Among the puzzles which remain is the asymmetry produced by certain projectiles (cone, teflon sphere). The conditions for the onset of rippling are also unclear; this could be clarified by independently controlling the velocity and size of the object.

We thank K. Reichard for the use of the hydrophone, B. Bitel for experimental assistance, and Qiang Du, A. Lyons, J. Roberts, E. Villermaux, and especially C. Clanet for helpful discussions. A. B. and J. B. K. would like to thank the Woods Hole Oceanographic Institution Geophysical Fluid Dynamics Summer Program (2006) for hospitality which led to the model. A. B. acknowledges the support of The National Science Foundation (CAREER Grant No. DMR-0094167).

*Also at: Department of Mechanical and Nuclear Engineering, Pennsylvania State University, University Park, PA, USA.
†Also at: Harvard School of Engineering and Applied Sciences, Harvard University, Cambridge, MA, USA.

[1] M. Minnaert, Philos. Mag. **16**, 235 (1933).
[2] H. C. Pumphrey, L. A. Crum, and L. Bjorno, J. Acoust. Soc. Am. **85**, 1518 (1989).
[3] A. Prosperetti and H. N. Õguz, Annu. Rev. Fluid Mech. **25**, 577 (1993).
[4] A. Mallock, Proc. R. Soc. A **95**, 138 (1918).
[5] A. M. Worthington, *A Study of Splashes* (Longman and Green, London, 1908).
[6] E. G. Richardson, Proc. Phys. Soc. London **61**, 352 (1948).
[7] J. Glasheen and T. McMahon, Phys. Fluids **8**, 2078 (1996).
[8] A. May, J. Appl. Phys. **23**, 1362 (1952).
[9] H. Shi, M. Itoh, and T. Takami, J. Fluids Eng. **122**, 806 (2000).
[10] L.-J. Leng, J. Fluid Mech. **427**, 73 (2001).
[11] B. Kersten, C. D. Ohl, and A. Prosperetti, Phys. Fluids **15**, 821 (2003).
[12] V. Duclaux, F. Caillé, C. Duez, C. Ybert, L. Bocquet, and C. Clanet, J. Fluid Mech. (to be published).
[13] R. Bergmann, D. van der Meer, M. Stijnman, M. Sandtke, A. Prosperetti, and D. Lohse, Phys. Rev. Lett. **96**, 154505 (2006).
[14] M. P. Brenner, S. Hilgenfeldt, and D. Lohse, Rev. Mod. Phys. **74**, 425 (2002).
[15] K. R. Weninger, H. Cho, R. A. Hiller, S. J. Putterman, and A. Williams, Phys. Rev. E **56**, 6745 (1997).
[16] N. Bremond, M. Arora, C.-D. Ohl, and D. Lohse, Phys. Rev. Lett. **96**, 224501 (2006).
[17] T. Truscott and A. Techet, Phys. Fluids **18**, 091113 (2006).
[18] G. Birkhoff and E. H. Zarantonello, *Jets, Wakes, and Cavities* (Academic, New York, 1957).
[19] A. May, J. Appl. Phys. **22**, 1219 (1951).
[20] D. Gilbarg and R. Anderson, J. Appl. Phys. **19**, 127 (1948).
[21] M. Lee, R. Longoria, and D. Wilson, Phys. Fluids **9**, 540 (1997).
[22] G. Eiffel, *La Résistance de l'Air et l'Aviation* (Dunod and Pinat, Paris, 1911).
[23] L. Rayleigh, Philos. Mag. **34**, 94 (1917).
[24] M. Strasberg, J. Acoust. Soc. Am. **25**, 536 (1953).
[25] H. I. Abelson, J. Fluid Mech. **44**, 129 (1970).
[26] J. B. Keller and I. I. Kolodner, J. Appl. Phys. **27**, 1152 (1956).
[27] A. Belmonte, T. Grumstrup, and J. B. Keller (to be published).
[28] D. Epstein and J. B. Keller, J. Acoust. Soc. Am. **52**, 975 (1972).